Polymer 51 (2010) 3486–3492

Contents lists available at ScienceDirect

Polymer

journal homepage: www.elsevier.com/locate/polymer

Structure and phase transition in thin films of block copolymer micelles complexed with inorganic precursors

Ae Jung Jang, Seung-kyu Lee, Seung Hyun Kim*

Division of Nano-Systems Engineering, Inha University, Incheon 402-751, South Korea

ARTICLE INFO

Article history:
Received 9 February 2010
Received in revised form
30 April 2010
Accepted 15 May 2010
Available online 31 May 2010

Keywords:
Block copolymers
Micelles
Nanocomposites

ABSTRACT

Block copolymer micelle can be used as nano-reactor where separated domains serve as a compartment for the production of nanomaterials, ultimately creating nanocomposite materials. In this work, thin nanocomposite films generated from polystyrene-*b*-poly(acrylic acid) (PS-*b*-PAA) micellar solution in which small amount of inorganic precursor was added were investigated. The films were prepared by spin coating onto silicon substrate, and then solvent-annealed. As-spun films exhibit typical micellar structure with spherical shape along which inorganic nanoparticles are dispersed. Such morphology remains unchanged after solvent annealing for micellar films with small amount of inorganic precursor. However, further increase in the amount of inorganic precursors brings about the morphological changes, producing different organization of inorganic nanoparticles in composite films. This behavior was found to strongly depend on the types of precursors and solvents used for annealing. These results illustrate a simple yet useful route to generate the polymeric nanocomposites with diverse structure and composition.

1. Introduction

Polymeric nanocomposites are commonly defined as a binary mixture of functional inorganic nanomaterials dispersed in a polymeric matrix. Inorganic materials with a characteristic size on the nanometer scale can give various functionalities with unique electric, magnetic, and optical properties while the polymer matrix allows the integration and stability of nanomaterials as well as processability. Moreover, nanocomposites of polymer and inorganic nanoparticles can exhibit new properties that are not possessed by the components in their own right. A large number of research works have been presented in the literature that were dedicated to technological and scientific problems of polymeric nanocomposites, and, as a result, the combination of such kinds of materials enables nanocomposites to be used in wide fields ranging from microelectronics to biomedical applications [1–13].

Synthesis of nanoparticles with uniform shape and size as well as effective control of spatial organization of nanoparticles are key in determining characteristics and applications of polymeric nanocomposites. Preparation of nanocomposites with well-dispersed nanoparticles in a matrix is still a challenge, requiring the development of new and more efficient fabrication methods. Among several strategies for the creation of such nanocomposites, block copolymer self-assembly can provide a very simple yet useful solution to overcome such problem, where block copolymers are used as a template to control size, shape, and organization of nanoparticles [14–19]. Block copolymer, composed of chemically distinct polymers connected by covalent bond, can spontaneously form well-defined, periodic nanostructures of which size and shape can be tuned by controlling the molecular weight of copolymer components and the composition of block copolymer. The domain size is set by the molecular size on the nanometer scale because the self-assembly of block copolymer is restricted by the connection of two blocks. Therefore, the nanostructures with regular periodicity based on the block copolymer self-assembly can provide inorganic nanomaterials with an ideal place for generation of well-dispersed nanocomposites. In effect, the incorporation of nanoparticles into block copolymer domains can be done in two ways [20]. In the first, the nanoparticles having uniform size and shape are synthesized separately and then mixed with block copolymer to generate polymeric nanocomposites. In this case, it is easy to control the shape and size of nanoparticles through separate synthesis, but difficult to make well-ordered dispersion in the polymer matrix due to the lack of interaction between nanoparticles and polymers. In order to improve the miscibility and dispersion of nanoparticles in the polymer matrix, another process to attach the functional group on

* Corresponding author. Tel.: +82 32 860 7493; fax: +82 32 873 0181.
E-mail address: shk@inha.ac.kr (S.H. Kim).

0032-3861/$ – see front matter © 2010 Elsevier Ltd. All rights reserved.
doi:10.1016/j.polymer.2010.05.024

the nanoparticle surface should be required in the most cases. In the other way, the inorganic precursors are mixed with block copolymer in solution, and then self-assembled together to form the nanocomposites with better dispersion of inorganic nanoparticles through reduction process. In this case, however, the reduction of inorganic precursors can sometimes destroy the dispersion of inorganic materials in the matrix, and it becomes difficult to control the size and shape of nanomaterials in the matrix.

In our work, block copolymer micelles are used as a template for composites to generate well-controlled, well-dispersed nanoparticles with uniform size and shape without severe aggregation of nanoparticles. Placed in a solvent where one segment is soluble and the other is not, the block copolymers will self-organize into supramolecular micelles with insoluble cores shielded from the solvent by a corona formed by the soluble segments. The use of block copolymer micelle as a tool of nanolithography has been intensively studied over the last decade since it can provide a simple, easy accessible route to generate nanostructured interfaces [21–25]. Another activity in block copolymer micelles finds their usage as nano-reactor where the micellar core can serve as a compartment for the production of inorganic nanomaterials [26–31]. In this work, the block copolymer micelles are used as a nano-reactor to produce uniform inorganic nanomaterials and to generate well-dispersed nanocomposites. Nanocomposite films are generated by using the micellar solution of block copolymers complexed with inorganic precursors, and then solvent-annealed for better organization. Solvent annealing technique was found to be able to create an array of micelles with long-range lateral order over large area [29]. Here, it is instead found that the morphological transition occurs through solvent annealing. Such behavior is observed to strongly depend on the concentration and type of inorganic materials and the solvent used for annealing. Consequently, it is demonstrated in our work that based on the block copolymer micelles, various patterns and dispersion of inorganic nanomaterials can be realized by controlling the solvent selectivity and interactions of inorganic precursors with components via selective complexation and solvent annealing.

2. Experimental section

2.1. Materials

The block copolymer used in this work was polystyrene-*block*-poly(acrylic acid) (PS-*b*-PAA) purchased from Polymer Source Inc. Its molecular weight and polydispersity are 20.3 kg mol^{-1} (M_{PS} = 16.0 kg mol^{-1} and M_{PAA} = 4.3 kg mol^{-1}) and 1.15, respectively. $HAuCl_4 \cdot 3H_2O$ and $AgNO_3$ were purchased as inorganic precursors from Sigma–Aldrich. All the solvents including toluene, THF, ethanol and dioxane were used without further purification.

2.2. Micelle formation and film generation

Two types of micelle were prepared by using different solvents in this work. Toluene, selective solvent for PS blocks, was used to produce the micelles with PAA blocks located in the core. In the second, the micelles with PAA blocks in the corona were produced by dissolving PS-*b*-PAA in THF and then adding ethanol dropwise that was selective for PAA blocks. After micelle formation, each micellar solution was mixed with predetermined amount of precursors to produce the complexation of inorganic precursor with block copolymer micelles.

The films were prepared by spin-coating the micellar solution on silicon substrates. Before use, the substrates were cleaned in piranha solution with 70/30 v/v of concentrated H_2SO_4 and H_2O_2 at 90 °C for 20 *min*, thoroughly rinsed with deionized water, and then blown dry with nitrogen gas. (***Caution****: Piranha solution reacts violently with organic compounds and should not be stored in a closed container.*) The film thickness was controlled by adjusting spinning speed and solution concentration. Spin-coated films were annealed in a saturated solvent vapor for 6 h.

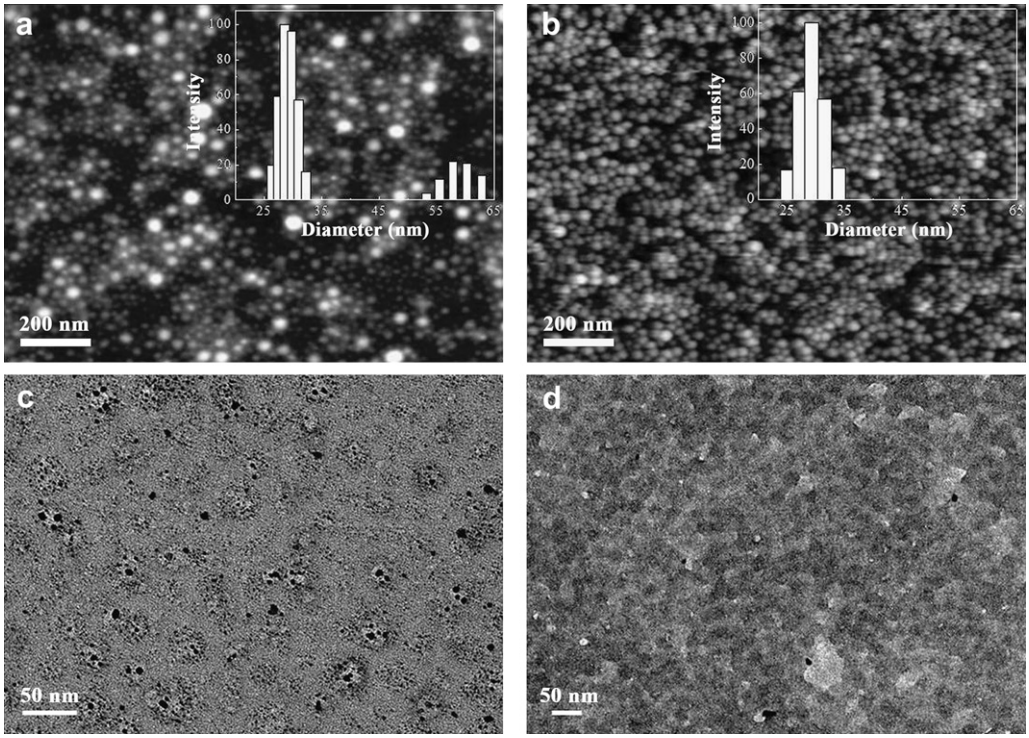

Fig. 1. SFM images (a, b), and TEM images (c, d) of PS-*b*-PAA micelles in toluene (a, c) and THF/ethanol (b, d), respectively. Size distribution of micelles in each solution by DLS is shown in the inset. TEM images were taken after the films were immersed in Au precursor solution.

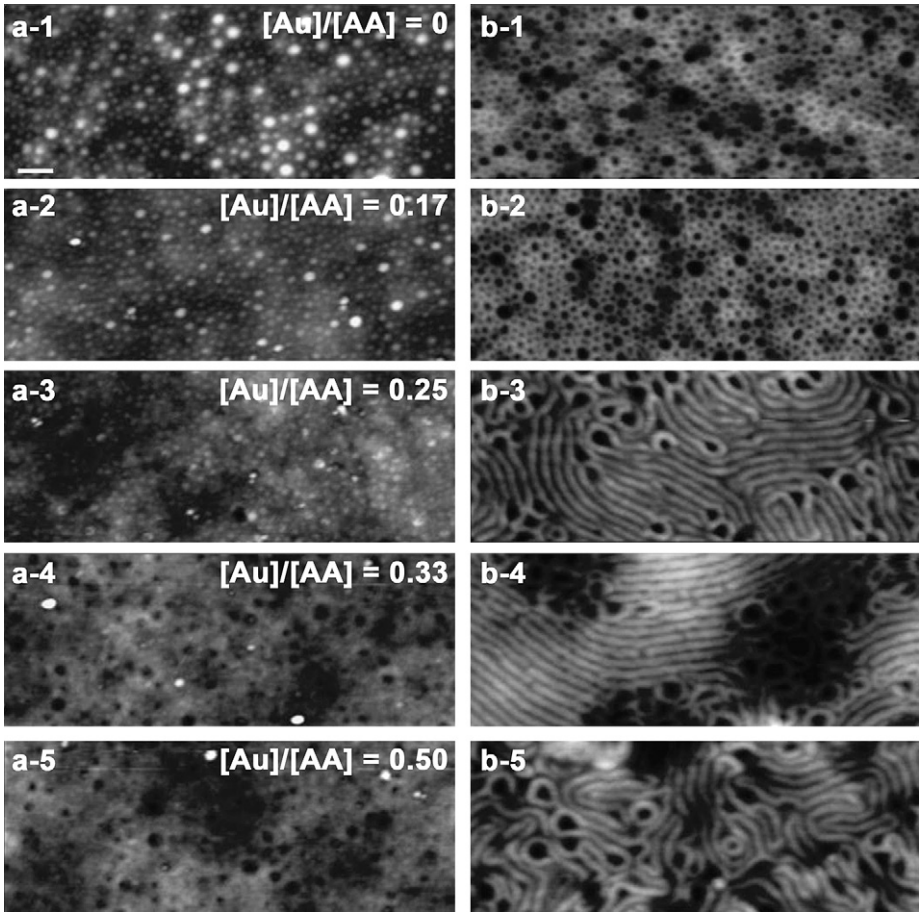

Fig. 2. SFM images of thin films of PS-*b*-PAA micelles complexed with different concentration of Au precursor in toluene before (a) and after (b) solvent annealing. The concentration of Au in micelles is expressed as a ratio of concentrations of Au to acrylic acid unit in PAA blocks, [Au]/[AA].

2.3. Characterization

The micellar solutions were characterized by dynamic light scattering (DLS) (90Plus/Brookhaven instruments corp.) with $\lambda = 658\ nm$ at a scattering angle of 90°. The surface and internal structures of the thin films were characterized by scanning force microscopy (SFM) in tapping mode and transmission electron microscopy (TEM). SFM used for characterization of surface morphology in this study was Veeco Nanoscope Multimode IVa Scanning Probe Microscope. TEM was performed on JEOL 100CS Electron Microscope operated at 120 kV to take images of the nanocomposites.

3. Results and discussion

PS-*b*-PAA block copolymer is a representative amphiphilic block copolymer of which micellar behavior has long been investigated in both regular and reverse forms by many research groups [27,32–34]. In an aqueous media, PS-*b*-PAA generates the normal micelles where insoluble hydrophobic PS blocks are located inside the core with hydrophilic PAA blocks comprising the corona while reverse micelles with a hydrophilic core are formed in organic solvents such as toluene. In this work, both types of micelles were prepared in toluene and THF/ethanol, respectively. In toluene which is a good solvent for PS blocks, the reverse micelles with PAA blocks in the core form, but the regular micelles with PS blocks in the core are produced in THF/ethanol solvent which is a selective solvent for PAA blocks. Both micellar solutions were spin-coated on the substrate to produce thin micellar films, and their morphologies were presented in Fig. 1. As shown in SFM images, both films exhibit typical micellar structure with spherical bumps on the surface. PS-*b*-PAA block copolymer is well-known to be able to form micelles with various morphologies ranging from spheres, rods, bicontinuous structures, vesicles, to even crew-cut structure depending on the copolymer composition [32,33]. However, for PS-*b*-PAA used in this work, only spherical micelles were observed in both the regular and reverse forms. The size and size distribution of micelles were measured by dynamics light scattering (DLS), and their results are displayed in the inset of the corresponding SFM images (Fig. 1(a) and 1(b)). The size of reverse micelles formed in toluene is more polydisperse, compared with that of regular micelles, showing two broad distributions. That was reflected in thin film morphology where the micelles with small and large sizes can be observed together, as shown in Fig. 1(a). If reverse micelles with larger size are eliminated in calculation of average size, both types of micelles exhibit very similar average size of 29.1 nm (reverse micelles) and 29.3 nm (regular micelles), respectively. To utilize the complexation ability of carboxylic acid units in PAA with inorganic precursors, thin films of PS-*b*-PAA micelles were immersed in Au precursor solution to load the gold nanoparticles into the PAA domains. As expected, the Au nanoparticles are observed in the core for reverse micelles (Fig. 1(c)), whereas they are dispersed in the matrix for regular micelles (Fig. 1(d)). These results confirm successful formation of reverse and regular micelles in toluene and THF/ethanol solvents, respectively.

In order to investigate the complexation effects of inorganic precursors on the structure of micellar films, small amount of Au precursors was added to the toluene solution of PS-*b*-PAA block copolymers with reverse micelles. Added Au precursors are

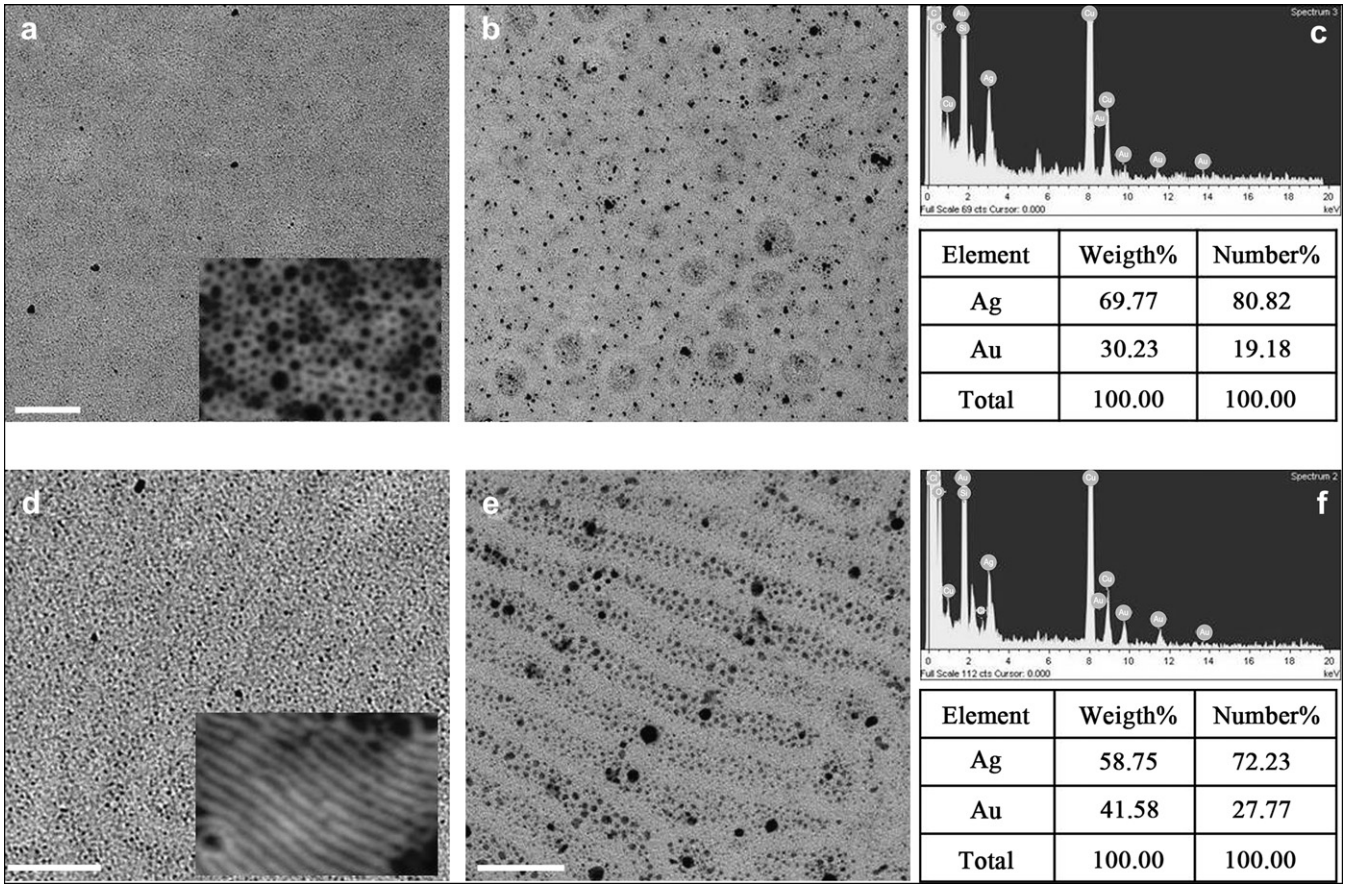

Element	Weigth%	Number%
Ag	69.77	80.82
Au	30.23	19.18
Total	100.00	100.00

Element	Weigth%	Number%
Ag	58.75	72.23
Au	41.58	27.77
Total	100.00	100.00

Fig. 3. Comparison of thin films of PS-*b*-PAA micelles with [Au]/[AA] = 0.17 (a,b,c) and 0.33 (d,e,f): (a, d) TEM images of thin films of PS-*b*-PAA micelles with [Au]/[AA] = 0.17 and 0.33; (b, e) TEM images and (c, f) EDX spectra of thin films of PS-*b*-PAA micelles with [Au]/[AA] = 0.17 and 0.33 after dipping in Ag precursor solutions.

expected to selectively complex with PAA blocks and located into micellar core. Surface structures of as-spun films of micellar solution containing Au precursors are shown in Fig. 2(a) where different number in each SFM image indicates the different concentration of Au precursor in micellar solution. The concentration of inorganic precursor was expressed as a molar ratio of Au ions to acrylic acid units and changed from [Au]/[AA] = 0 to [Au]/[AA] = 0.5. At lower concentration of Au precursor loaded, typical structure of micellar films is observed as in the case without Au precursors. The micellar films with higher content of Au precursors (Fig. 2(a-4) and (a-5)) appear to show slightly different surface structure but they also have the micellar features in thin films as the micelle formation in solution was indeed confirmed by DLS measurement. According to DLS data, the average size of micelles in solution was increased from 29.1 nm at [Au]/[AA] = 0 to 52.9 nm at [Au]/[AA] = 0.5. Similar structure was observed for as-spun films of normal micelles in THF/ethanol when they were complexed with Au precursors. However, in this case, the average micellar size showed no change with increasing the concentration of Au precursor in solution, but exhibited constant micelle size at all the Au precursor concentrations.

In the SFM images in Fig. 2(b) are shown the effects of solvent annealing for the micellar films of PS-*b*-PAA complexed with Au precursors, where dioxane was used as a solvent for annealing. Based on the solubility parameter [35], dioxane is more selective for PAA blocks than for PS blocks. Depending on the concentration of Au precursors, the effects of solvent annealing appear differently. At lower concentration of Au precursors, as can be seen in Fig. 2(b-1) and (b-2), solvent annealing induces open-up (sometimes called cavitation) of micelles at the film surface, producing the hole structure at the surface. This process allows PAA blocks to be exposed to the surface and thus to be available for further reaction through conjugation. However, at higher concentration of precursors, different structure is generated, that is, the morphological transformation from the spherical to cylindrical shapes occurs after solvent-annealing under dioxane vapor. This may be caused by the changes in volume fraction of block component domains and the balanced interactions of Au precursor and solvent with block copolymers, which will be discussed in detail later. The effects of nanoparticles addition on the structure of block copolymers have been investigated by several groups [36–41]. Some have focused on the location of added nanoparticles within block copolymer domains [36–38], and others have observed the nanoparticle-induced phase transition of block copolymers [38–41]. Recently, it was reported that the morphology in block copolymer films were varied in depth by adding high concentration of nanoparticles. This behavior was found to be due to the volume change of nanoparticles along the depth direction caused by the selectivity of solvent. However, such spatial variation of morphology was observed only for thick films, but not expected for thin films containing one or two layers of micelles, as in our case. The same morphological transformation at higher concentration of Au precursor was observed for thicker films with thickness of about 150 nm or more, showing thickness-independent behavior over the range covered in our work. On the other hand, the same annealing experiments have been conducted for PS-*b*-PAA micellar films formed from THF/ethanol solution. In this case, the cavity of micellar cores only was observed but the morphological transition

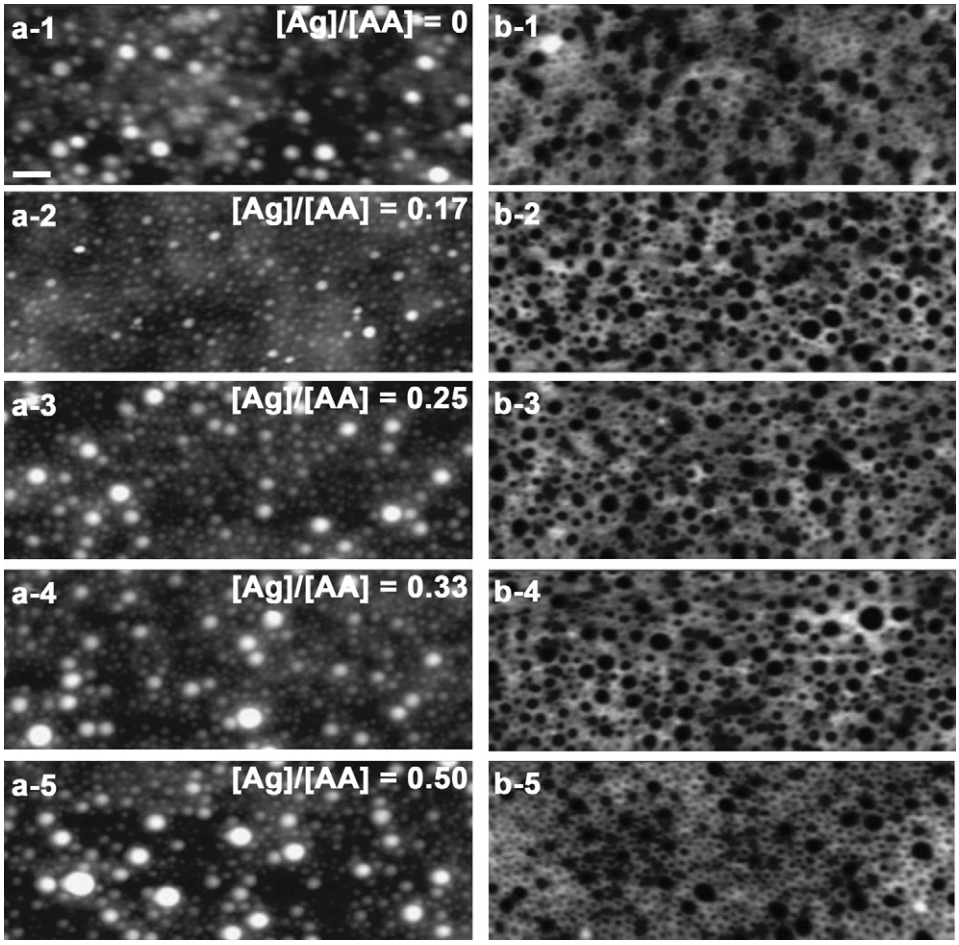

Fig. 4. SFM images of thin films of PS-*b*-PAA micelles complexed with different concentration of Ag precursor in toluene before (a) and after (b) solvent annealing. The concentration of Ag in micelles is expressed as a ratio of concentrations of Ag to acrylic acid unit in PAA blocks, [Ag]/[AA].

did not happen even at higher concentration of gold precursor for limited annealing time. Although there may be still possibility that the morphology would be transformed at even longer annealing time, that's out of scope here and so we will only concentrated on the reverse micelles in the rest part of the paper.

Fig. 3 shows the TEM images of thin micellar films complexed with Au precursors of different concentrations that directly exhibit the formation and organization of the Au nanoparticles in the polymeric matrix. Contrary to our expectation, few gold nanoparticles were seen in TEM images, as shown in Fig. 3(a) and (d). Even after dipping the micellar films in the Au precursor solution in ethanol, any appreciable increase of the gold nanoparticles in the film was not observed (data not shown here), although we managed to identify the location of nanoparticles within block copolymer structure in Fig. 1 through prolonged dipping. But, when dipped in the Ag precursor solution, the PS-*b*-PAA micellar films were observed to load large amount of Ag nanoparticles along the PAA microdomains. At lower concentration of Au precursor loaded (Fig. 3(b)), the Ag nanoparticles are dispersed in the micellar core with spherical shape. On the other hand, the Ag nanoparticles were found to be loaded into the cylindrical PAA domains, as shown in Fig. 3(e). These results clearly show the phase transition of PAA domains through complexation and solvent annealing, and also reveal that PAA blocks have stronger interaction with Ag precursor than with Au precursors. The presence of both Au and Ag nanoparticles in the micellar films was confirmed by EDX analysis in Fig. 3(c) and (f). Relative amount of Au and Ag nanoparticles in the films is tabulated below the EDX spectra, showing that more Ag nanoparticles are presented along the PAA microdomains. Consequently, these results show that different types of nanoparticles can simultaneously be loaded in the same domains by using different loading methods in sequence.

When Ag precursor instead of Au precursor were added to PS-*b*-PAA micellar solution and complexed with PAA blocks before spin-coating, the different change in thin film structure from the case of Au precursor was observed after solvent annealing, as demonstrated in Fig. 4. Before annealing, the micellar films complexed with Ag precursor have spherical micelles of which size increases with increasing the concentration of Ag precursor, as in the case of Au precursor. However, such spherical shapes are found to remain unchanged in thin films after solvent annealing even at high concentration of Ag precursor within block copolymer, and only burst-out of the micelles occurs, producing the holes at the film surface. This may be due to stronger interaction of Ag precursor with PAA blocks, compared with Au precursor. In general, it is known that Ag^+ ions in $AgNO_3$ strongly interactions with carboxylic acid groups in PAA blocks while $AuCl_4^-$ from $HAuCl_4$ in solution form weak coordination interaction with COOH group. Such strong interaction forces the aggregation of PAA blocks with Ag precursor to maintain their morphology in spite of the increase in the volume fraction of PAA domains during solvent annealing.

The morphological transformation by solvent annealing also exhibits the strong dependence of type of solvent used for annealing. As can be seen in Fig. 5 where Au precursor was complexed with PAA blocks in solution, when a solvent selective for PAA blocks such as dioxane and THF was used for annealing, the

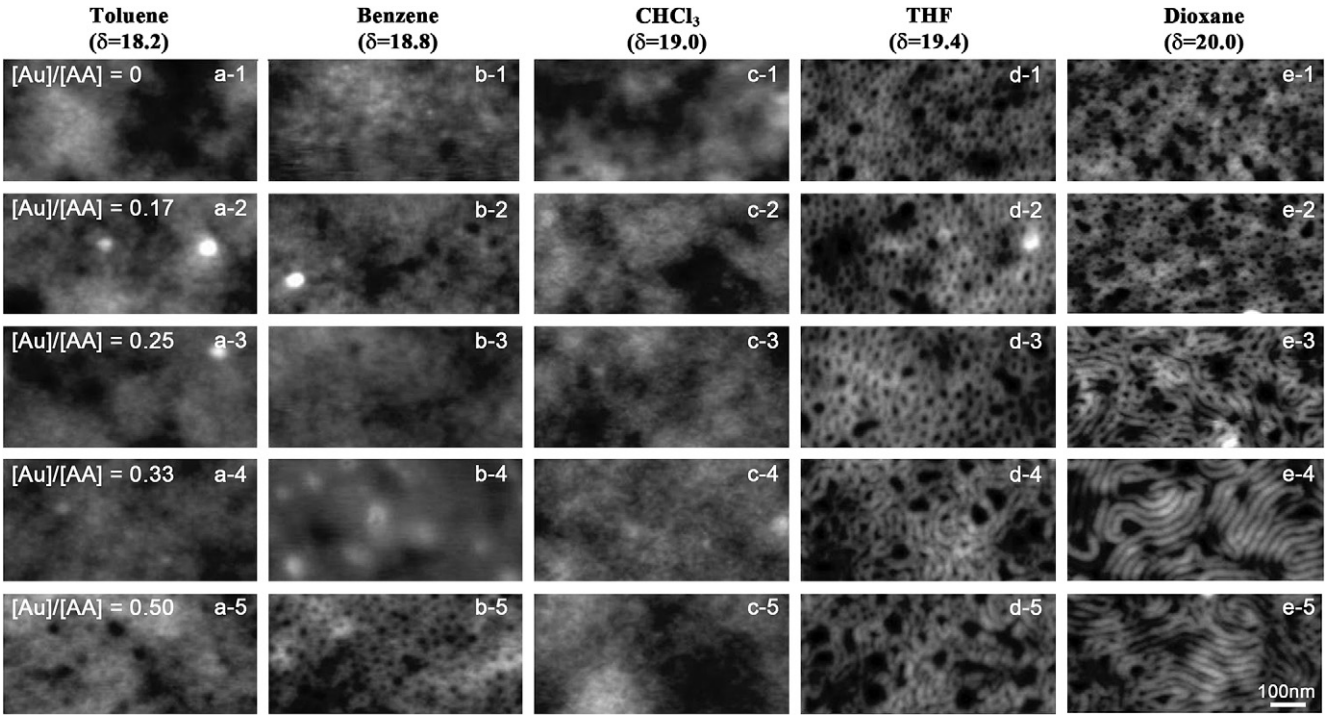

Fig. 5. SFM images of thin films of PS-*b*-PAA micelles annealed in different solvent vapors of (a) toluene, (b) benzene, (c) $CHCl_3$, (d) THF, and (e) dioxane. Each micelle was complexed with different concentrations of Au precursor in toluene as denoted in each figure from [Au]/[AA] = 0–0.50.

morphology changes from spheres to cylinders after solvent annealing at higher content of Au precursor. However, as the solubility parameter of solvent decreased and its selectivity changed from PAA to PS blocks, such morphological transformation was not observed even at higher concentration of Au precursor with [Au]/[AA] = 0.5. Instead, featureless structure with no surface patterns was formed where PS blocks would be expected to cover the entire film surface due to lower surface tension of PS and selectivity of solvent used. These results indicates that the interaction of solvent with block copolymer also have strong effects on the structure of micellar films through solvent annealing.

All the results shown above can be understood as follows by considering the volume change of PAA block domains induced by addition of inorganic precursors and the interactions of both inorganic precursors and solvents with copolymer components. When Au precursors are dissolved in PS-*b*-PAA micellar solution in toluene, Au precursors are selectively complexed with PAA blocks and loaded into the micellar core, leading to the increase in average micellar size as well as in volume fraction of PAA blocks. Such increase in the volume fraction by loading Au precursors is further amplified by use of selective solvent for PAA blocks during solvent annealing. More solvent molecules are absorbed in the PAA domains than in PS domains, leading to further increase in the volume fraction of PAA domains and finally inducing the morphological transformations from spherical to cylindrical structures. For morphological changes, the assistance from solvents selective for PAA blocks should be required to further increase the volume fraction of PAA domains. When neutral or selective solvents for PS blocks are used on annealing, the increase in volume fraction of PAA domains in the PS matrix is not so enough to invoke the morphological transformation in the concentration range of inorganic precursor added in this work, instead the micellar films keep their original structure during solvent annealing or exhibit the surface structure with no patterns after solvent annealing because the film surface is covered by the PS blocks. However, when the precursor having stronger interactions with PAA blocks such as Ag precursor are added, the micellar aggregation maintains its original shape even under solvent vapor selective for PAA blocks, due to the strong interaction between PAA blocks and Ag precursors. All these results suggest that the block copolymer micelle complexed with inorganic precursor can offer the templates for generation of polymeric nanocomposites having various shapes and structures by appropriately choosing the types of solvents and inorganic precursors. Moreover, by using two different routes for loading the inorganic precursors into block copolymer domains at the same time, two different types of inorganic nanoparticles can be loaded into the same domain simultaneously. However, in order to further improve the uniformity in size and shape of inorganic nanoparticles within the copolymer microdomains, although severe aggregation of inorganic nanoparticles were avoided by using the block copolymer micelles as a template, controlled reduction process should be added in our work.

4. Conclusion

We have demonstrated that block copolymer micelles in thin films can effectively act as a template to produce well-controlled nanocomposites with various structures through complexation with inorganic precursors and solvent annealing. Choosing appropriate types of inorganic precursors and solvents for annealing and controlling their concentration enable various nanostructures and shapes in the micellar films to be realized in a simple way for just one block copolymer system. Here, when Au precursors were selectively complexed with PAA blocks in PS-*b*-PAA block copolymer, the micellar film showed spherical structure at lower concentration of Au precursor but exhibited the morphological change from spherical to cylindrical nanostructure at higher concentration of Au nanoparticles after solvent annealing under dioxane vapor. However, different results were observed when Ag precursor was added to the micellar solution or different solvents were used for solvent annealing. Such behavior results from the balance of relative change in volume fraction of copolymer

components and interaction of inorganic precursors and solvents with block components. Moreover, two different routes to load the inorganic precursors were applied for one micellar film to be able to generate two different types of nanoparticles simultaneously within the same domains in one diblock copolymer system.

This strategy to use the micellar films as a template for generation of nanocomposites is quite general and will be expected to be applied for any micellar system of block copolymers by selecting appropriate types of inorganic precursors and solvents. This can provide a very simple route to produce well-defined, well-organized nanocomposites with various patterns and organization in thin films.

Acknowledgements

This work was financially supported by Basic Science Research Program through the National Research Foundation of Korea (NRF) grant funded by the Ministry of Education, Science, and Technology (MEST) (No. 313-2008-2-D01270).

References

[1] Mai Y-W, Yu Z-Z. Polymer nanocomposites. Cambridge: Woodhead Publishing Ltd.; 2006.
[2] Paul DR, Robeson LM. Polymer 2008;49(15):3187–204.
[3] Ramesh GV, Porel S, Radhakrishnan TP. Chem Soc Rev 2009;38(9):2646–56.
[4] Wu YY, Cheng GS, Katsov K, Sides SW, Wang JF, Tang J, et al. Nat Mater 2004;3(11):816–22.
[5] Reiss G, Hütten A. Nat Mater 2005;4(10):725–6.
[6] Sun S. Adv Mater 2006;18(4):393–403.
[7] Holder E, Tessler N, Rogach AL. J Mater Chem 2008;18(10):1064–78.
[8] Niu DC, Li YS, Qiao XL, Li L, Zhao WR, Chen HR, et al. Chem Commun 2008;37:4463–5.
[9] Klem MT, Young M, Douglas T. Mater Today 2005;8(9):28–37.
[10] Dobson J. Nanomedicine 2006;1(1):31–7.
[11] Gu H, Xu K, Xu C, Xu B. Chem Commun 2006;9:941–9.
[12] Lin XM, Samia ACS. J Magn Magn Mater 2006;305(1):100–9.
[13] Mornet S, Vasseur S, Grasset F, Veverka P, Goglio G, Demourgues A, et al. Prog Solid State Chem 2006;34(2–4):237–47.
[14] Sun SH, Anders S, Hamann HF, Thiele JU, Baglin JEE, Thomson T, et al. J Am Chem Soc 2002;124(12):2884–5.
[15] Rutnakornpituk M, Thompson MS, Harris LA, Farmer KE, Esker AR, Riffle JS, et al. Polymer 2002;43(8):2337–48.
[16] Sanchez C, Julian B, Belleville P, Popall M. J Mater Chem 2005;15(35–36):3559–92.
[17] Bockstaller MR, Mickiewicz RA, Thomas EL. Adv Mater 2005;17(11):1331–49.
[18] Balazs AC, Emrick T, Russell TP. Science 2006;314(5802):1107–10.
[19] Pyun J. Polym Rev 2007;47(2):231–63.
[20] Grubbs RB. J Polym Sci Pol Chem 2005;43(19):4323–36.
[21] Glass R, Moller M, Spatz JP. Nanotechnology 2003;14(10):1153–60.
[22] Gorzolnik B, Mela P, Moeller M. Nanotechnology 2006;17(19):5027–32.
[23] Kronholz S, Rathgeber S, Karthauser S, Kohlstedt H, Clemens S, Schneller T. Adv Funct Mater 2006;16(18):2346–54.
[24] Lohmueller T, Bock E, Spatz JP. Adv Mater 2008;20(12):2297-+.
[25] Wang Y, Becker M, Wang L, Liu JQ, Scholz R, Peng J, et al. Nano Lett 2009;9(6):2384–9.
[26] Spatz JP, Herzog T, Mossmer S, Ziemann P, Moller M. Adv Mater 1999;11(2):149–53.
[27] Bennett RD, Miller AC, Kohen NT, Hammond PT, Irvine DJ, Cohen RE. Macromolecules 2005;38(26):10728–35.
[28] Haryono A, Binder WH. Small 2006;2(5):600–11.
[29] Yun SH, Il Yoo S, Jung JC, Zin WC, Sohn BH. Chem Mat 2006;18(24):5646–8.
[30] Meli L, Li Y, Lim KT, Johnston KP, Green PF. Macromolecules 2007;40(18):6713–20.
[31] Pietsch T, Gindy N, Fahmi A. Polymer 2008;49(4):914–21.
[32] Zhang LF, Eisenberg A. Science 1995;268(5218):1728–31.
[33] Zhang LF, Eisenberg A. J Am Chem Soc 1996;118(13):3168–81.
[34] Boontongkong Y, Cohen RE. Macromolecules 2002;35(9):3647–52.
[35] Brandrup J, Immergut EH, Grulke EA. Polymer handbook. Hoboken: John Wiley & Sons, Inc.; 1999.
[36] Bockstaller MR, Lapetnikov Y, Margel S, Thomas EL. J Am Chem Soc 2003;125(18):5276–7.
[37] Chiu JJ, Kim BJ, Kramer EJ, Pine DJ. J Am Chem Soc 2005;127(14):5036–7.
[38] Thompson RB, Ginzburg VV, Matsen MW, Balazs AC. Science 2001;292(5526):2469–72.
[39] Huh J, Ginzburg VV, Balazs AC. Macromolecules 2000;33(21):8085–96.
[40] Kim BJ, Chiu JJ, Yi GR, Pine DJ, Kramer EJ. Adv Mater 2005;17(21):2618-+.
[41] Matsen MW, Thompson RB. Macromolecules 2008;41(5):1853–60.